phys. stat. sol. (a) **86**, 295 (1984)

Subject classification: 18.4; 21.4

Laboratoire Louis Néel, C.N.R.S., Grenoble[1]) *(a)*
and Departamento de Optica y Estructura de la Materia,
Facultad de Ciencias, Santander (b)

Magnetic Structure of the Er_2Pt Antiferromagnet

By

D. GIGNOUX (a), J. C. GOMEZ-SAL (b), and J. RODRIGUEZ FERNANDEZ (b)

By means of neutron diffraction the magnetic structure of the Er_2Pt, antiferromagnet ($T_N = 9$ K), space group Pnma is studied. The magnetic cell ($2a, b, c$) is twice the crystallographic one. A reduction of the magnetic moments is observed because of the crystal field effects. Magnetic atoms are divided into four sublattices. This leads to a non collinear magnetic structure with different easy magnetization directions, which originate from the strong magnetocrystalline anisotropy in compounds with very low symmetry.

Mittels Neutronenbeugung wird die magnetische Struktur von Er_2Pt, einem Antiferromagnet ($T_N = 9$ K), Raumgruppe Pnma, untersucht. Die magnetische Zelle ($2a, b, c$) ist die zweifache kristallographische Zelle. Eine Reduzierung des magnetischen Moments wird auf Grund der Kristallfeldeffekte beobachtet. Die magnetischen Atome sind in vier Untergitter geteilt. Dies führt zu einer nichtkollinearen magnetischen Struktur mit unterschiedlichen Richtungen der leichten Magnetisierbarkeit, was von der starken magnetokristallinen Anisotropie in Verbindung mit sehr niedriger Symmetrie herrührt.

1. Introduction

The R_2Pt compounds (R rare earth) crystallize in the orthorhombic Ni_2Si-type structure [1]. The magnetic properties of these compounds have been recently studied [2]. From Gd to Ho they are ferromagnetic with Curie temperatures between 155 K (Gd_2Pt) and 17 K (Ho_2Pt). Er_2Pt and Tm_2Pt have an antiferromagnetic behaviour, with Néel temperatures of 9 and 5 K, respectively. In Fig. 1, we present the magnetization curves of Er_2Pt at different temperatures. Below T_N metamagnetic transitions are observed at 4.2 and 7 K, around 12 kOe.

The magnetic structure of the Tb_2Pt [3] ferromagnet was investigated recently. A complex non-collinear structure was found and narrow walls between magnetic domains were observed at very low temperatures. These magnetic properties result from competition between indirect exchange interactions and large magnetocrystalline anisotropy.

In order to determine the magnetic structure of Er_2Pt we have performed neutron diffraction experiments that are presented in this paper.

2. Experimental

The erbium and platinum used were 99.9 and 99.99% pure, respectively. Polycrystalline samples were induction melted in a cold crucible. No extra phase was observed as far as could be seen by the Debye-Scherrer pattern. Neutron diffraction experiments were performed at the Centre d'Etudes Nucléaires of Grenoble (C.E.N.G.) at 4.2 and 77 K.

[1]) 25, Avenue des Martyrs, 166X, 38042 Grenoble Cédex, France.

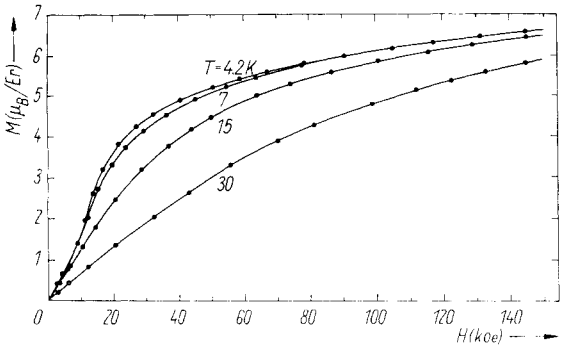

Fig. 1. Field dependence magnetization of Er_2Pt at different temperatures; $T_N = 9$ K

3. Crystallographic Structure

The orthorhombic structure of Er_2Pt belongs to the Pnma space group. The lattice parameters of the orthorhombic cell which contains four formula units are $a = 0.7037$ nm, $b = 0.4705$ nm, and $c = 0.8668$ nm. All the atoms lie in the 4c site with m(C_s) symmetry. The positions of the four atoms in this site are (1) in $(x, 1/4, z)$; (2) in $(-x, 3/4, -z)$; (3) in $(1/2 - x, 3/4, 1/2 + z)$, and (4) in $(1/2 + x, 1/4, 1/2 - z)$. In Fig. 2a, we present the neutron diffraction pattern performed at 77 K, i.e. above the Néel temperature.

The observed peaks are characteristic of the Ni_2Si structure and can be indexed with the parameters listed before. Selection rules of the crystallographic Pnma group are satisfied: the Bragg peaks $(h, k, 0)$ with $h = 2n + 1$ and $(0, k, l)$ with $k + l = 2n + 1$ do not appear. The intensities were calculated with the Fermi lengths $b_{Er} = 0.79 \times 10^{-12}$ cm and $b_{Pt} = 0.95 \times 10^{-12}$ cm.

We have refined the atomic positions comparing the calculated and observed intensities which are presented in Table 3. The reliability factor is, $R = |I_{obs} - I_{cal}|/I_{obs} =$

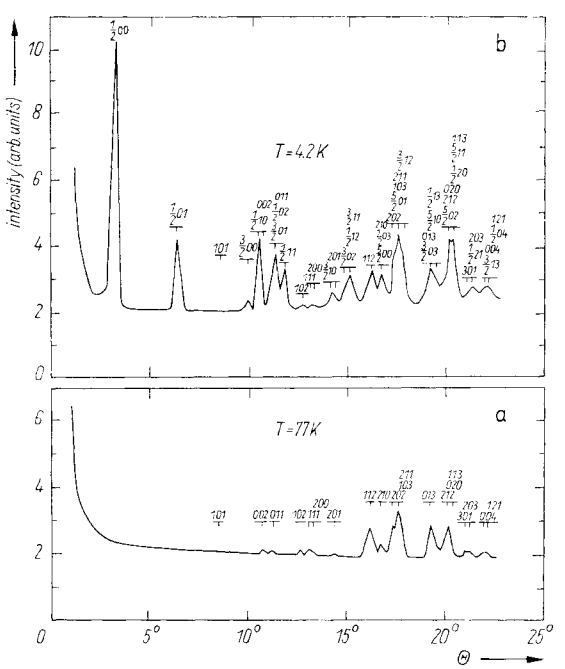

Fig. 2. Er_2Pt neutron diffraction patterns at 77 and 4.2 K ($\lambda = 0.162$ nm) (θ is the Bragg angle)

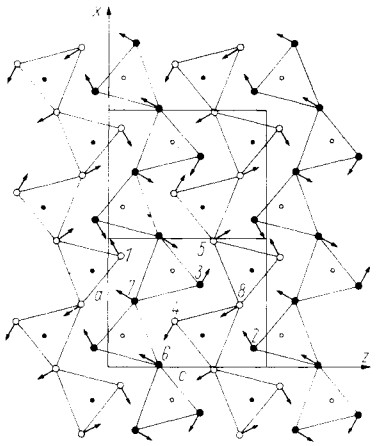

Fig. 3. Magnetic structure of Er_2Pt. $y = 1/4$: ○ Er, ○ Pt; $y = 3/4$: ● Er, ● Pt

Table 1

Positions of the eight erbium and four platinum atoms in Er_2Pt

atoms	x	z
Er(I): 1, 2, 3, 4	0.860	0.080
Er(II): 5, 6, 7, 8	0.988	0.671
Pt	0.248	0.094

= 4.45%, and the atomic positions are reported in Table 1; they are close to those determined in Gd_2Pt [1] and Tb_2Pt [3]. The crystallographic structure of Er_2Pt is shown in Fig. 3.

4. Magnetic Structure

At 4.2 K, the neutron diffraction pattern (Fig. 2b) exhibits a set of new peaks, which are indexed in a magnetic cell of parameters ($2a$, b, c). The propagation vector of the magnetic structure is then $\boldsymbol{k} = (1/2, 0, 0)$. No increase of the intensity of the nuclear peaks is observed.

In order to determine the possible configuration of the magnetic moments, we used the macroscopic method proposed by Bertaut [4], which allows to select the different possible configurations of the magnetic moments, and which apply when the main contribution to the magnetic energy is of second order. We must determine the irreducible representation of the Pnma group, G_k, associated with the propagation vector $\boldsymbol{k} = (1/2, 0, 0)$. We choose as generating elements of the Pnma group, the screw axis 2_{1x} at (x, 1/4, 1/4) and 2_{1z} at (1/4, 0, z) and the inversion centre $\bar{1}$ at (0, 0, 0). The other five elements of the Pnma group are: the identity E, the screw axis $2_{1y} = 2_{1x}2_{1z}$ at (1/2, y, 0), and the mirrors, $n_x = 2_{1x}\bar{1}$ at (1/4, y, z); $m_y = 2_{1y}\bar{1}$ at (x, 1/4, z), and $a_z = 2_{1z}\bar{1}$ at (x, y, 1/4). The elements of this G_k, Pnma group associated with $\boldsymbol{k} = (1/2, 0, 0)$ do not commute, and only two irreducible representations of second order appear. In Table 2 we show the irreducible representations and their basis vectors for the two different sites.

The basis vectors associated with the Γ_1 representation are in the b-direction and they cannot account for the observed intensities of the (1/2, 0, 0) and (3/2, 0, 0) peaks, which have a very simple expression for the magnetic structure factors. Then the basis vectors of the two sites belong to the Γ_2 representation and the moments must be in the (x, z) plane, however in this representation a lot of possibilities remain possible. A refinement of the magnetic intensities for each possibility led to the basis vectors: A_{Ix} and G_{Iz} for the Er(I) atoms and A_{IIx} and F_{IIz} for the Er(II) atoms. The components of the magnetic moments of the two erbium sites, which gave the best agreement between the observed and the calculated intensities (Table 3), are reported in Table 4. The moments on each site are very close ($m_I = 5.6\mu_B$ and $m_{II} = 6.0\mu_B$). The resulting magnetic structure is shown in Fig. 3. From all the refinements performed

Table 2

Representations and basis vectors associated with $k = (1/2, 0, 0)$ vector of the Pnma group. The atoms are in 4c site

representations	symmetry elements							basis vectors	
	E	2_{1x}	2_{1z}	2_{1y}	$\bar{1}$	n_x	a_z	m_y	site I, atoms (1, 2, 3, 4)	site II, atoms (5, 6, 7, 8)
Γ_1	$\begin{pmatrix}1&0\\0&1\end{pmatrix}$	$\begin{pmatrix}0&1\\\bar{1}&0\end{pmatrix}$	$\begin{pmatrix}1&0\\0&\bar{1}\end{pmatrix}$	$\begin{pmatrix}0&\bar{1}\\\bar{1}&0\end{pmatrix}$	$\begin{pmatrix}0&1\\1&0\end{pmatrix}$	$\begin{pmatrix}1&0\\0&\bar{1}\end{pmatrix}$	$\begin{pmatrix}0&1\\\bar{1}&0\end{pmatrix}$	$\begin{pmatrix}\bar{1}&0\\0&\bar{1}\end{pmatrix}$	$\begin{pmatrix}C_{Iy}\\F_{Iy}\end{pmatrix}$ $\begin{pmatrix}A_{Iy}\\-G_{Iy}\end{pmatrix}$	$\begin{pmatrix}C_{IIy}\\F_{IIy}\end{pmatrix}$ $\begin{pmatrix}A_{IIy}\\-G_{IIy}\end{pmatrix}$
Γ_2	$\begin{pmatrix}1&0\\0&1\end{pmatrix}$	$\begin{pmatrix}0&1\\\bar{1}&0\end{pmatrix}$	$\begin{pmatrix}1&0\\0&\bar{1}\end{pmatrix}$	$\begin{pmatrix}0&\bar{1}\\\bar{1}&0\end{pmatrix}$	$\begin{pmatrix}0&\bar{1}\\\bar{1}&0\end{pmatrix}$	$\begin{pmatrix}\bar{1}&0\\0&1\end{pmatrix}$	$\begin{pmatrix}0&\bar{1}\\1&0\end{pmatrix}$	$\begin{pmatrix}1&0\\0&1\end{pmatrix}$	$\begin{pmatrix}C_{Ix}\\-F_{Ix}\end{pmatrix}$ $\begin{pmatrix}A_{Ix}\\G_{Ix}\end{pmatrix}$ $\begin{pmatrix}F_{Iz}\\-C_{Iz}\end{pmatrix}$ $\begin{pmatrix}G_{Iz}\\A_{Iz}\end{pmatrix}$	$\begin{pmatrix}C_{IIx}\\-F_{IIx}\end{pmatrix}$ $\begin{pmatrix}A_{IIx}\\G_{IIx}\end{pmatrix}$ $\begin{pmatrix}F_{IIz}\\-C_{IIz}\end{pmatrix}$ $\begin{pmatrix}F_{IIz}\\A_{IIz}\end{pmatrix}$

Table 3

Observed and calculated neutron diffraction intensities at 77 and 4.2 K in Er_2Pt

				77 K			4.2 K			
h	k	l	θ	I^N_{cal}		I^N_{obs}	I^m_{cal}		$I^m_{cal} + I^N_{cal}$	I_{obs}
1/2	0	0	3.30	0		0	48.7		48.7	45.5
1/2	0	1	6.30	0		0	13.4		13.4	25.0
1	0	1	8.53	0.4		0	0		0.4	0
3/2	0	0	9.94	0		0	6.0		6.0	10.1
0	0	2	10.77	4.0	4.0	5.2	0	113.0	117.0	115.7
1/2	1	0	10.46	0			113.0			
0	1	1	11.30	2.9			0			
1/2	0	2	11.28	0	2.9	3.2	87.9	98.1	101.0	104.8
3/2	0	1	11.32	0			10.3			
1/2	1	1	11.78	0		0	85.6		85.6	81.5
1	0	2	12.68	6.4		9.0	0		6.4	9.0
1	1	1	13.13	10.3	13.4	13.4	0	0	13.4	13.4
2	0	0	13.31	3.1			0			
2	0	1	14.39	4.2	4.2	4.2	0	20.0	24.2	35.7
3/2	1	0	14.11	0			20.0			
3/2	0	2	14.74	0			5.3			
1/2	1	2	15.10	0	0	0	39.5	175.0	175.0	184.8
3/2	1	1	15.14	0			130.2			
1	1	2	16.20	152.8		145.0	0		152.8	145.0
2	1	0	16.71	47.7			0			
1/2	0	3	16.63	0	47.7	48.0	56.1	108.7	156.4	143.2
5/2	0	0	16.72	0			52.6			
2	0	2	17.25	48.2			0			
2	1	1	17.59	210.0			0			
1	0	3	17.64	42.4	300.6	307.9	0	189.8	490.4	500.2
5/2	0	1	17.61	0			56.5			
3/2	1	2	17.89	0			133.3			
0	1	3	19.21	202.8			0			
3/2	0	3	19.22	0	202.8	211.6	4.4	75.2	278.0	291.9
1/2	1	3	19.51	0			58.3			
5/2	1	0	19.59	0			12.5			
2	1	2	20.05	15.0			0			
0	2	0	20.14	203.0			0			
1	1	3	20.40	13.3	228.3	226.0	0	163.8	392.1	408.4
5/2	0	2	20.07	0			6.8			
5/2	1	1	20.37	0			79.7			
1/2	2	0	20.43	0			77.3			
3	0	1	20.96	64.1			0			
2	0	3	21.27	36.4	100.5	85.4	0	55.1	155.6	132.7
1/2	2	1	21.19	0			55.1			
0	0	4	21.95	55.0			0			
1	2	1	22.02	0.8	55.8	60.9	0	100.9	156.7	155.3
3/2	1	3	21.81	0			94.5			
1/2	0	4	22.22	0			6.4			
					$R = 4.57\%$				$R = 5.73\%$	

for the other possibilities belonging to Γ_2 we can assure that the proposed model is the only one which accounts for the observed magnetic intensities.

Table 4
Characteristics of the magnetic structure of Er_2Pt

atoms	basis vectors	$M_x(\mu_B)$	$M_z(\mu_B)$	$\|M\|$ (μ_B)	angle with $0x$ axis
Er(I) 1, 2, 3, 4	(A_x, G_z)	4.8	2.9	5.6	$-31.7°$
Er(II) 5, 6, 7, 8	(A_x, F_z)	3.0	5.2	6.0	$60.6°$

5. Discussion

The antiferromagnetic structure of Er_2Pt is complex and non-collinear. All the moment lie in the mirror plane perpendicular to the [0, 1, 0] direction. The magnetic cell is twice the crystallographic one. In the (x, z) plane four easy magnetization directions appear, moments of 1 and 2 are perpendicular to those of 6 and 7: from one cell to the other along a, the moments of two atoms lying in the same position are antiparallel, leading to the antiferromagnetic character of this compound. This type of double cell antiferromagnetic structures was found also in rare earth–aluminium [5] intermetallic compounds. Because of the difference of surroundings arising from the low symmetry, the magnetic atoms are divided into various sublattices with different easy magnetization directions. The complex magnetic structure of Er_2Pt results from a competition between the strong magnetocrystalline anisotropy and long-range exchange interactions.

The magnetic moment in zero applied field, determined by neutron diffraction, reaches only $5.6\mu_B$ and $6.0\mu_B$ for each site, respectively, values which are smaller than the free Er^{3+} one $(9\mu_B)$. This reduction is similar to that observed in Tb_2Pt $(5.6\mu_B)$ and is a result of the crystal field effects. The surrounding of the atoms of each site being different the reduction of the magnetic moment by the crystal field can be different. This is confirmed by a crystal field calculation that we have performed in the over-simplified point charge model.

All these properties confirm again [6, 7] the important role of the crystal field effects in the compounds with low symmetry.

References

[1] J. LE ROY, J. M. MOREAU, D. PACCARD, and E. PARTHE, Acta cryst. **B34**, 9 (1978).
[2] A. CASTETS, D. GIGNOUX, J. C. GOMEZ-SAL, and F. RODRIGUEZ-GONZALEZ, Solid State Commun. **45**, 993 (1983).
[3] A. CASTETS, D. GIGNOUX, J. C. GOMEZ-SAL, F. RODRIGUEZ-GONZALES, and E. ROUDANT, phys. stat. sol. (a) **73**, 475 (1982).
[4] E. F. BERTAUT, Acta cryst. **A24**, 217 (1968).
[5] C. BÈCLE, R. LEMAIRE, and D. PACCARD, J. appl. Phys. **41**, 855 (1970).
[6] B. BARBARA, D. GIGNOUX, D. GIVORD, F. GIVORD, and R. LEMAIRE, Internat. J. Magnetism **4**, 77 (1973).
[7] D. GIGNOUX, F. GIVORD, R. LEMAIRE, and J. C. GOMEZ-SAL, Proc. 12th Rare Earth Res. Conf. **1**, 57 (1976).

(Received July 17, 1984)